Gene expression programming for green synthesis of silver nanoparticles: Size evolution

Amineh Shafaei[1], Gholam Reza Khayati*[1, 2]

[1]*Department of Materials Science and Engineering, Faculty of Engineering, Shahid Bahonar University of Kerman, Kerman, Iran;*
[2]*Mahani Mathematical Research Center, Shahid Bahonar University of Kerman, Kerman, Iran.*

ABSTRACT

In this study, gene expression programming (GEP) was used as a new method for the formulation of the size of silver nanoparticles (AgNPs) as functions of the $AgNO_3$-to-opium syrup (OS) ratio, pH, temperature (T), agitation speed (AS) and feed rate (Fr) of reducing agent in green synthesis. The models differ from each other concerning their genes number, chromosomes, interconnected function, and head size. A total of 63 samples were selected at different practical parameter products to generate databases for the new particle size formulations, testing, and training sets. The training and testing sets included 47 and 16 randomly selected mixtures for the proposed models. The best GEP model is found, and this final model can predict the size of AgNPs with a correlation coefficient (R^2) of 0.828, a root means square error (RMSE) of 5.894, a root relative squared error (RRSE) of 0.44. All results in the models indicated an applicable performance for predicting the minimum particle size of the AgNPs and found it reliable. The predicted model showed that all of the input parameters affect the resulting particle size. GEP modeling results denoted that the selected GEP successfully predicts the behavior of the size of nanoparticles as functions of operating variables.

Keywords: Gene expression programming; Green synthesis; Silver nanoparticles; Modeling

1. Introduction

Today, nanotechnology has a special application in medicine for making metal nanoparticles with a minimum size. There are several methods for making nanoparticles. In physical and chemical methods [1-3], which are the common routes of nanoparticle synthesis, the use of toxic substances is inevitable. Therefore, there is an urgent need to develop green synthesis methods for metal nanoparticles [4, 5]. An attractive approach to achieve this aim is to exploit the potential of biological resources in nature. Over the years, fungi, bacteria, viruses, and plants have been used to make non-toxic nanoparticles at a lower cost and save more energy

[6, 7]. The size of nanoparticles affects their unique properties, especially in the medical field. The size of synthesized nanoparticles, composition, structure, and morphology obtained due to the choice of extract plays a significant role in affecting their unique properties. Also, It should be noted that the role of opioids, including OS, which contains natural compounds, all act as analgesic neurotransmitters in the body that reduce pain in the body by affecting the central nervous system. In this regard, they are used in medicine [8-10]. Therefore, finding a way to determine the desired properties of AgNPs by considering experimental parameters in a way that achieves the minimum size is very important.

So, finding accurate modeling to predict the size of nanoparticles is very useful [3, 11].

GEP has an inherent ability to model the engineering problems. The main advantages of GEP are the acceptable accuracy, easy to implement and does not require to the complex problem-solving procedures [12-14]. To the best of our knowledge, various methods have been used to predict the size of nanoparticles. However, modeling the effect of practical parameters and predicting the size of AgNPs with the help of opium syrup (OS) by GEP method has not been studied yet. In summary, the main contributions of this study are: (i) providing of an accurate model based on experimental date of green synthesis of AgNPs using OS by GEP; (ii) consideration of practical parameteres including $AgNO_3$-to-OS ratio, AS, Fr of OS, pH, and T as inputs and the the size of AgNPs as output of GEP model, and (iii) usage of sensitivity analysis to investigate and ranke the effect of each input variable on the size of AgNPs.

2. Experimental

OS-mediated bio-reduction is prepared by mixing OS with $AgNO_3$. The preparation of nanoparticles takes place at different T and completes in 30 minutes.

2.1. Synthesis of AgNPs

To synthesis AgNPs, 1 mM solution of $AgNO_3$ (Merck 99.99 wt.% purity) as precursor and OS as reducing agent were used. The AgNPs were prepared using OS because of their medicinal properties. OS was prepared by International food service distributors association (IFDA) company. NaOH (98 wt.% purity), HNO_3 (65 wt.% purity) as adjusting of pH were supplied by Merck. A solution of 100 mL $AgNO_3$ 1 mM was prepared at first. Adding OSs to 100 mL of 1 mM $AgNO_3$ provided various concentrations of reactants. In this study, evaluation of several important experimental factors, including volume ratio ($AgNO_3$-to-OS ratio as a reducing agent) of 20:1, 10:1, 20:3 and 5:1, Fr of 0.33, 0.66, 2 and 10 (mL/min), AS = 100, 250, 300, 500 and 600 rpm, pH = 5 to 8 and T = 25, 37, 50 and 65 °C were studied as inputs and AgNPs size as output. This setup was incubated in a dark chamber to minimize photo-activation of silver nitrate at different T. The changed color of the solution confirmed the reduction of Ag^+ to Ag^0 from colorless to dark brown. The reduced solution was centrifuged at 15000 rpm for 20 min. The prepared AgNPs washed three times using the centrifugation process and deionized water and dried for further analysis. Due to the wide range and many affecting parameters, a test, called factorial D-optimal array, was designed and carried out to decrease the experiment data. The number of trials that were equal to 1280 trials in full factorial design decreased to 63 trials without declining the quality of data. In the synthesis of 63 trials, the duration of 30 min is considered (Table 1). For training and testing each GEP, these data were randomly divided into the training and testing sections. Accordingly, 47 schedules were applied for training, whereas 16 ones were used for testing. For training and testing of each GEP model, collected data randomly divided into two sections, including 47 and 16 trials. The former section was applied for training, and the latter section was used for testing.

2.2. Characterization of AgNPs

The structures, phase analysis, and the average particle size of biosynthesis AgNPs were examined by X-ray diffraction (XRD) (Philips, X'pert-MPD system at 30 mA and 40 kV by Cu-Kα radiation) in 2θ between 30º and 90º. Scherer's equation [15] was employed to calculate the size of AgNPs [16, 17]. Further analysis of morphology and size of prepared samples were done using transmission electron microscopy (TEM) (PHILPS EM-208S) and environmental scanning electron microscope (ESEM) analysis. Moreover, the chemical point analyses were determined using energy dispersive spectroscopy (EDS) (Silicon Drift 2017, USA). Dynamic light scattering (DLS) (Malvern Ltd., Malvern, UK) was utilized to determine the distribution of the prepared sample. DLS analysis was carried out using distilled water at 25 °C, viscosity 0.8872 cP, and a refractive index of 1.33 as the solvent.

3. Definition of predictive model
3.1. Genetic programming (GP)

Systems, artificial neural networks, GP, superficial logic, and adaptive neural-fuzzy logic are common soft techniques that are preferred if the amount of data available is appropriate. GP has only recently commenced to correctly formulate the properties and efficiency of engineering materials [18, 19]. GP is a pioneering learning method that uses Darwin's theory to derive a symbolic regression model. Using intrinsic complexity to solve the problem distinguishes GP from other methods of using artificial intelligence for modeling. For example, machine learning solutions such as neural networks

Table 1- Experimentally data series for the preparation of AgNPs by green synthesis

| NO	AgNO3/ OS (mL or CC)	Fr (mL/min)	pH	T (°C)	AS (rpm)	NO	AgNO3/ OS (mL or CC)	Fr (mL/min)	pH	T (°C)	AS (rpm)	NO	AgNO3/ OS (mL or CC)	Fr (mL/min)	pH	T (°C)	AS (rpm)
G1	5	10	8	25	250	G22	6.66	0.33	5	37	300	G43	20	0.33	5	37	100
G2	20	0.66	6	37	300	G23	10	0.33	5	37	300	G44	10	0.66	6	37	100
G3	5	2	7	37	300	G24	6.66	10	7	50	500	G45	20	0.33	5	25	100
G4	5	0.33	6	50	300	G25	20	10	7	50	500	G46	5	10	8	25	100
G5	10	2	8	50	300	G26	6.66	0.66	8	65	600	G47	5	0.66	7	25	100
G6	20	2	8	65	300	G27	5	0.66	8	65	600	G48	20	2	8	65	250
G7	5	0.33	8	25	500	G28	6.66	2	6	25	250	G49	5	2	6	25	100
G8	5	0.66	7	37	600	G29	10	10	6	65	600	G50	20	2	8	50	100
G9	20	0.33	7	50	600	G30	10	0.66	8	65	600	G51	5	0.66	5	65	100
G10	5	2	5	65	600	G31	5	0.33	5	37	300	G52	5	0.66	7	25	100
G11	10	0.33	7	65	600	G32	5	0.66	6	37	300	G53	5	2	6	25	100
G12	20	0.66	8	65	600	G33	20	0.66	6	37	250	G54	5	0.66	5	65	100
G13	20	0.33	5	37	300	G34	5	2	7	37	250	G55	5	2	7	50	300
G14	10	0.66	6	37	300	G35	5	0.33	6	50	250	G56	20	0.66	7	25	600
G15	10	0.66	6	25	300	G36	10	2	8	50	250	G57	5	0.33	6	65	250
G16	6.66	2	7	25	300	G37	5	0.66	5	65	250	G58	5	0.33	8	65	300
G17	6.66	0.33	6	65	300	G38	6.66	2	5	50	100	G59	5	0.33	8	25	100
G18	10	10	5	37	600	G39	20	0.33	7	50	100	G60	10	0.66	7	37	250
G19	6.66	0.33	8	37	600	G40	6.66	10	6	65	100	G61	20	2	6	50	100
G20	6.66	10	8	37	100	G41	10	0.33	7	65	100	G62	5	10	5	25	250
G21	10	0.66	6	25	500	G42	20	0.66	8	65	100	G63	10	0.33	8	65	100
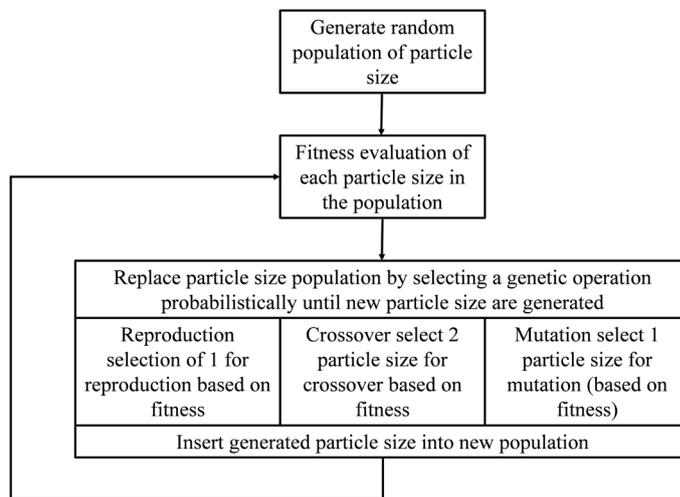
Fig. 1- GP structure.

and genetic algorithms (GA) use the form or scope of predetermined solutions [20]. GP, firstly proposed by Koza [21], takes its power from the biological natural selection system and automatically solves problems using a computer. The GP selects a population for modeling and then uses a random combination of chromosomes to find a more consistent state.

The GP initializes a population and compounds the chromosomes known as random members. Then, considering the degree of consistency of the predicted data with the experimental data (or fitness function) as a criterion, the optimal state of the combination of chromosomes is selected. Figure 1 presents the schematic of GP.

GP consists of combining various mathematical functions (power, sqrt, sin, tan, cos, log, ln) and operators (+, -, /) simultaneously to find the solutions. It is able to solve the problem while improving the program architecture of the general practitioner. In this study, empirical formulas were used for the prediction of the particle size of $AgNO_3$. GP aims to find a program that matches the experimental results well. This side of the program is very important for catching the nearest solution. GP creates the first population randomly from the previously defined space. GP gives a program as an output to the user [22].

3.2. GEP

GEP is an advanced version of GP that allows the use of various forms encoded in the fixed-length linear chromosomes with computer programs in various sizes and shapes. In other words, genes are used as smaller chromosome components to encode subroutines. Besides, the function and structure of linear chromosomes provide significant capabilities to the important genetic operators, including transposition, recombination, and mutation [12-14]. A significant advantage of GEP is that, given the sequence of a gene, it allows inferring exactly the phenotype and vice versa. It is known as the Karva language. In this language, it is possible to define the number of genes, the type of linker function, and the length of genes as a priori for each problem. The expression tree is the other approach in GEP to illustrate the output.

3.3. GEP structure and parameters

The experimental data used for the modeling of the particle size of AgNPs. If d_0, d_1, d_2, d_3, d_4, and d_5 are input variables and the particle size is as output, the hidden functions connecting these variables are the major task in GEP. The formulas obtained by GEP can be used for estimating the relationship between the characteristics of the particle size of AgNPs. The variables of the GEP models were presented in Table 2.

The database (63 experiments in Table 1) is randomly divided into testing (47 experiments) and training (16 experiments) section [23] and used to construct the models. It is important to note that the proposed GEP models are valid only in the range of data collected in Table 2.

3.4. GEP formulations

Table 3 shows selected GEP parameters in this study using Gene Xpro Tools 5.00 software. As can be seen, chromosome number 30 has the best performance in GEP-1 to GEP-6 models to predict the AgNPs. Explicit formulations based on the GEP-1 to GEP-6 approach models for the size of AgNPs were obtained by consideration of $AgNO_3/OS$, AS (rpm), Fr (mL/min), T (°C), and pH as effective parameters. The obtained related formulations of GEP-1 to GEP-6 models are in accordance with Table 4.

3.5. Evaluating the training of the GEP model

In order to investigate the performance of the extracted equation using the GEP method, the accuracy was estimated using statistical indices including R^2, RMSE, RRSE, and mean absolute error (MAE) (Eqs. 1-4) [24]:

$$R^2 = 1 - \frac{\sum_i (t_i - p_i)^2}{\sum_i (p_i)^2} \tag{1}$$

$$RMSE = \frac{1}{n} \sum_i \frac{|t_i - p_i|}{t_i} \times 100 \tag{2}$$

$$RRSE = \sqrt{\frac{\sum_i (t_i - p_i)^2}{\sum_i (t_i - \left(\frac{1}{n}\right)\sum_i t_i)^2}} \tag{3}$$

$$MAE = \frac{1}{n} \sum_i |t_i - p_i| \tag{4}$$

In which, n is the total number of datasets, t_i is measured values and p_i is predicted values.

Theoretically, the model with an R squared near 1 and error indices (RMSE, RRSE, and MAE) closer to zero has higher performance. Table 5 summarized these indices.

Table 2- The variables of the GEP models

Code	Input variable	Min	Max	Code	Output variable	Range (nm)
d_0	AgNO₃/Opium	5	20			
d_1	Fr (mL/min)	0.33	10			
d_2	pH	5	8	y	Particle size (nm)	9-57
d_3	T (°C)	25	65			
d_4	AS (rpm)	100	600			

Table 3- GEP parameters used to construct the models

GEP parameters definition	Choice
Function set	+,-,/,*,exp(x),Ln(x),1/x,x^2,x^1/3,avg(x), arctan(x),tan(x),1-x
Number of Chromosomes	30
Head size	8
Number of genes	3
Number of generation	487226
Linking function	Addition
Fitness Function error type	RRSE
Mutation rate	0.00546
Inversion rate	0.00546
One-point recombination rate	0.00277
Two-point recombination rate	0.00277
Gene recombination rate	0.00277
Gene transposition rate	0.00277
IS Transpositon	0.00546
RIS Transposition	0.00546
Trainig samples	47
Testing samples	16
Training fitness	708.563
Maximum fitness	1000
Constants per gene	10

Table 4- Explanation of mathematical equations for various GEP approaches

Models	Predict equation
GEP-I	$y=\exp((((-7.17)+((9.87)^2-d[3]))/(\log(d[4]))^2))+((((d[2]+(((((-4.41)+d[0])/2)+((-1.32)*6.42))/2))/2)-6.42))^2+ (1-((1-(\tanh(d[1])*(7.36 -d[1])))/(1-(1/(3.49)))))$
GEP-II	$y=\text{Log}((1/((((((3.96*-24.83)+((-11.27+d[4]/2))/2)+(2.07+d[3]))/2))^2)+(((8.42+2.450-((2.26+d[2]))^2)-((1/(d[1]))+d[1]))+(((1-(1/(d[1])))-(d[0]*1.08))+(((d[2]+d[2])/2)*(-1.23*-1.23)))$
GEP-III	$y=((1-(-7.80-(((d[2])2)-25.65)/(d[3]+d[3]))))^2)+((1-((d[2]*6.96)-2.66))-((1/(d[1]))-(1-d[0])))+((((d[4]/d[1])+d[3])*d[1])/((-5.59-d[3])-(-3.98/d[1])))$
GEP-IV	$y=(((((-6.70-5.72)*-6.70)-(-2.73+d[0]))-d[2])-6.70)+((((d[4]*-19.98)-(d[3]*d[3]))))^{1/3})-((3.82*d[2])-(d[1]/-0.61)))+(((-4.30/-1.53)+(-8.48*d[1]))*((d[0]*1.33)+(-4.35*d[2]))))^{1/3}$
GEP-V	$y=(1-((1-((9.46*3.77)+(1.15-D[0])))-\text{Atan}((6.96-d[0]))))+((((d[4]^{1/3})^2+(\exp(d[1])))/4.83))^{1/3}+\exp(((1-((d[2]-8.06))^{1/3}) - 8.28/((-6.01+d[3])/2))))$
GEP-VI	$y=\text{Arctan}(gepmax2((\exp 8.11)-((d[4]*d[0])+10.24)), 1.56))+\text{Arctan}((\exp ((gepmax2 (d[2], 7.46)-d[2]))*((-5.94*d[2])/d[0]-d[3]))))+(\exp(\text{Arctan}((d[0]*d[1])))-(gepmin2(((d[1]+d[0])/2),d[0])+(-9.94-10.08)))$

Table 5- Summaries of statistical indices including R^2, RRSE, RMSE, and MAE values for 6 most appropriate GEP models

No.	R^2		Error						
			Training			Testing			
	Training	Testing	RRSE	MAE	RMSE	RRSE	MAE	RMSE	
GEP-1	0.832	0.828	0.411	3.507	5.108	0.44	4.796	5.894	
GEP-2	0.788	0.77	0.461	4.149	5.728	0.505	5.416	6.754	
GEP-3	0.815	0.66	0.43	3.635	5.341	0.62	6.47	8.285	
GEP4	0.77	0.773	0.481	4.632	5.977	0.523	5.789	6.987	
GEP-5	0.758	0.796	0.492	4.115	6.108	0.465	4.875	6.219	
GEP-6	0.836	0.692	0.404	3.771	5.024	0.575	6.173	7.681	

3. 6. Tree structure of GEP

The output of models made by GEP can be expressed using two different languages. Gene language and ET language. These languages allow the user to recognize the sequence of genes, which is referred to as the Karva symbol [24]. As an example in Figure 2 the tree structures for estimating the grain size is shown.

3. 7. Sensitivity analysis

One of the effective methods to determine the effect of each input parameter on the selected output is the use of sensitivity analysis. The purpose of the analysis was to reduce the number of input parameters so that they do not measure the performance of the model. Reducing input parameters leads to a reduction in unnecessary data collection, resulting in lower costs. A step-by-step approach to the GEP trained was performed by changing each input parameter once at a constant rate to apply the sensitivity analysis. Different constant rates (5, 10) are selected in this article. For each input parameter, the percentage in the output was modified as the input parameter was changed. The sensitivity of each of the input parameters was calculated by the following equation (5) [25]:

$$S_i(\%) = \frac{1}{N}\sum_{j=1}^{N}\left(\frac{\%change\ in\ output}{\%change\ in\ input}\right)_j \qquad (5)$$

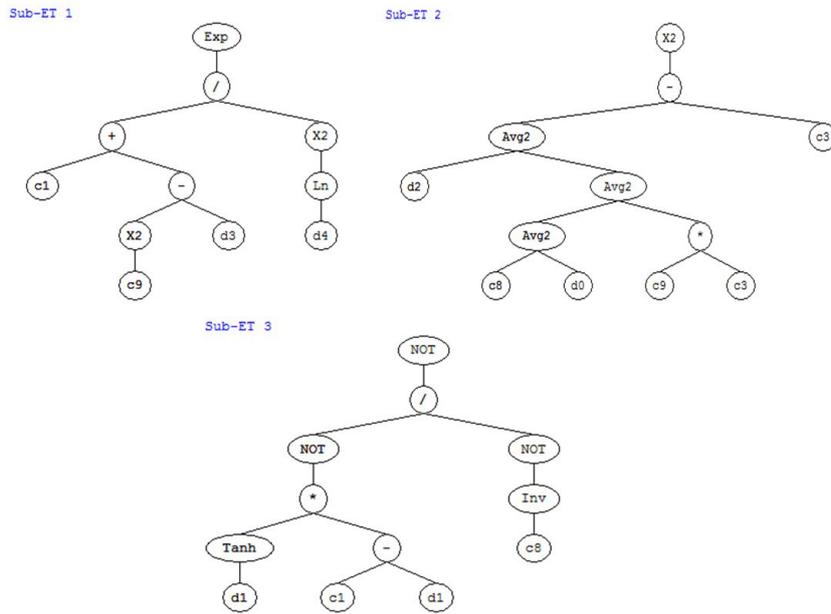Where S_i is the sensitivity level (%).

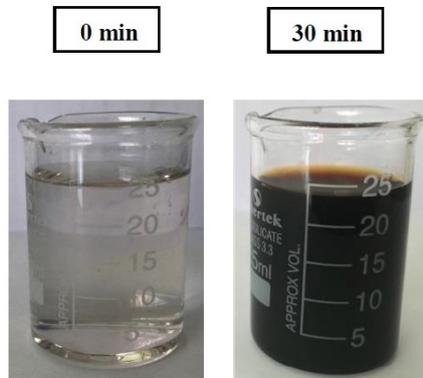Fig. 2- An example of tree structure in GEP.

Fig. 3- Example of time-dependent color changes of colloidal silver precursor after the addition of OS within the data collection prepared in sample 17.

Fig. 6-

4. Results and discussion

By adding different concentrations of OS to the AgNO$_3$ (mentioned in section 2.1), the reduction reaction was performed after 30 min in all samples, and over time, the color of the samples changed from colorless to dark brown (Figure 3). These color changes can be related to the excitation of surface plasmon vibrations in AgNPs due to AgNO$_3$ reduction to Ag^0.

The morphological character of AgNPs synthesized using OS was showed by the ESEM image. Figure 4 (a) shows that they had spherical shapes. Figure 4 (c) shows the presence of silver in the synthesized composition, which confirms the

synthesis of AgNPs, and its maximum absorption is about 3 keV. From EDS spectra, it is clear that the AgNPs were reduced by OS. The analysis also confirmed the presence of O, C, and N, elements which are the main constituents of OS that adsorbed to the surface of nanoparticles. The TEM micrograph of AgNPs is shown in Figure 4 (b), which demonstrates spherical shape agglomerated clusters and narrow particle size distribution. DLS analysis in Figure 4 (d) showed that the size distribution of AgNPs synthesized based on the concentration of 1 mM silver nitrate solution was between 5 to 68 nm.

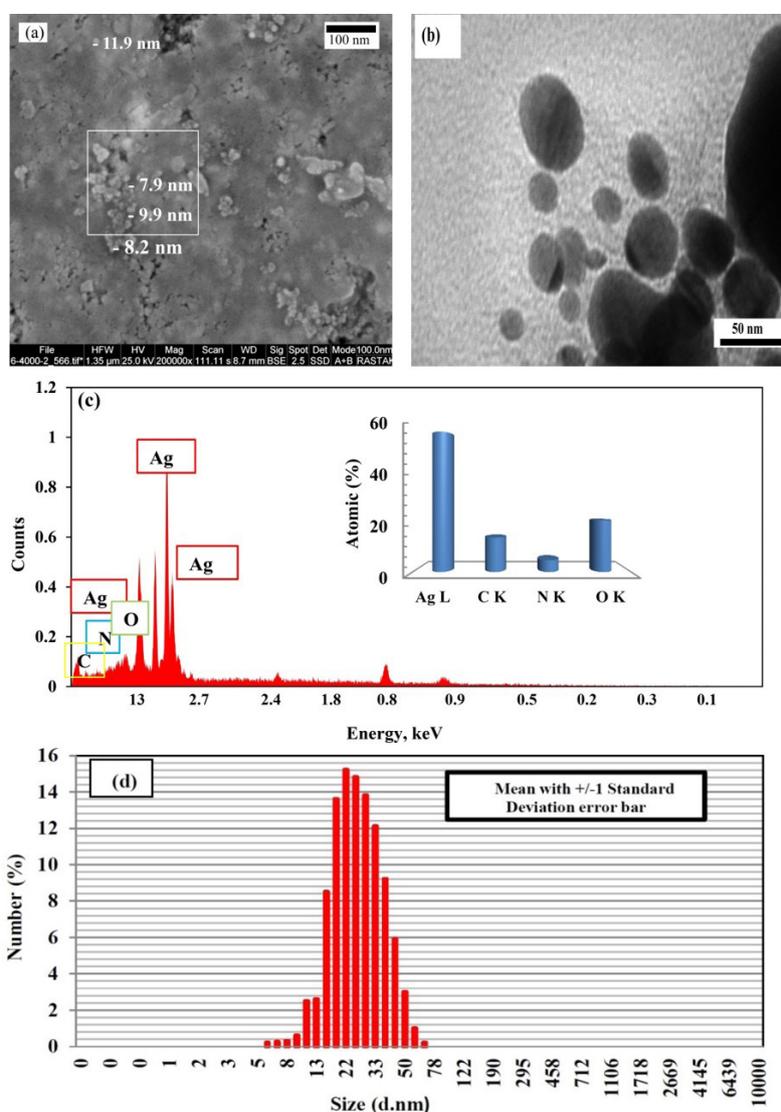As an example, Figure 5 confirms the evolution

Fig. 4- (a) ESEM image (b) TEM image (c) EDS spectrum, (d) DLS of green synthesized AgNPs prepared in sample 17.

of peaks at 2θ = 38.13 °, 44.31 °, 64.56 °, 77.51 °, and 81.62 °, corresponding to the crystalline plates (111), (200), (220), (311) and (222) of Ag phase with FCC structure, respectively, in accordance with Ag (Code number 00-004-0783). The average size of AgNPs was estimated by the Scherrer equation to be about 33 nm (sample 17 in Table 1). It should be noted that all the size of AgNPs is shown schematically in Figure 6.

In this study, the GEP model contains three genic chromosomes linked to each other by the addition (+) function. The expression tree of each gene (sub- ETs) is shown in Figure 2, that the general relationships between them are extracted as an equation given in Table 4.

Figure 7 shows a good agreement between the experimental results and the values predicted by the GEP model. It can be inferred that the proposed model was able to model the relationship between the selected operational parameters with the low-error output and relatively high correlation in the training phase (Figure 7a). Similar behavior was repeated in the testing step (Figure 7 (b)). Therefore, it can be concluded that the model could
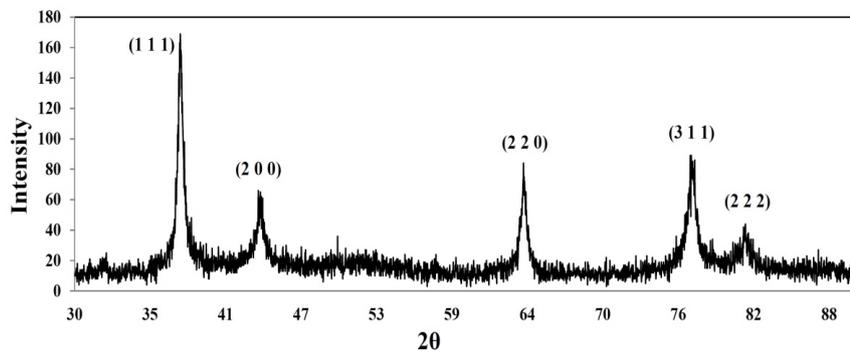

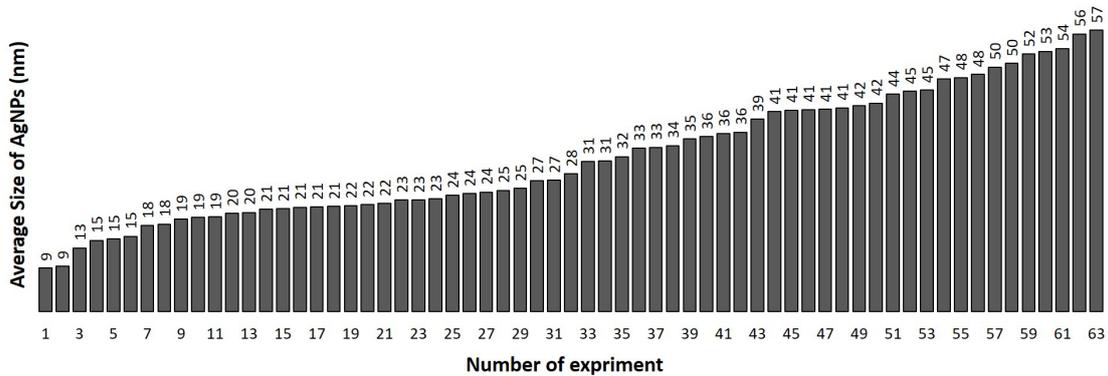Fig. 5- XRD spectra of AgNPs using OS prepared prepared in sample 17.

Fig. 6- Changes of the average particle size of Ag prepared prepared using OS as a reducing agent calculated by Scherer equation.
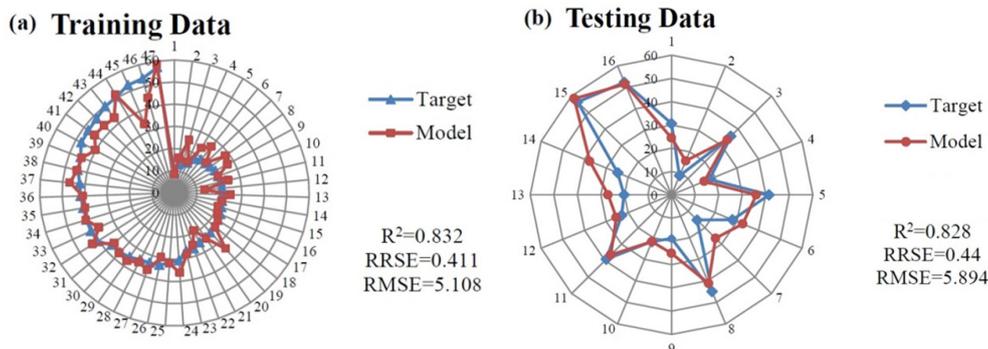

Fig. 7- Comparison of experimental data obtained from the model in two steps (a) training and (b) testing based on GEP-I.

effectively predict the size of nanoparticles in both stages. The R^2, MAE, RRSE, and RMSE values are shown in Table 5 for the training and testing data.

Figure 8 compared the accuracy of the most appropriate 6 GEP with each other. As shown by consideration of various statistical indices, the best GEP was changed. In this regard for the RRSE, RMSE, R^2, and MAE values respectively proposed the GEP (6 Train & 1 Test) and GEP (1 Train & 1 Test) as the most appropriate GEP model. Accordingly, consideration of errors or R^2 individually cannot be utilized as a criterion for selecting the best-proposed model.

In order to solve this issue, the fitness value (Eq. 6) is defined, which is a combined form of errors and R^2 as the threshold.

$$Fitness\ value = RMSE + RRSE + MAE + 1/(R)^2 \quad (6)$$

As shown, lower fitness values indicate better fitness. Figure 9 compared the fitness value of various investigated GEP.

Figures 10 (a-j) shows a three-dimensional diagram based on the interaction of experimental parameters on nanoparticle size using the regression equation. It should be noted that the
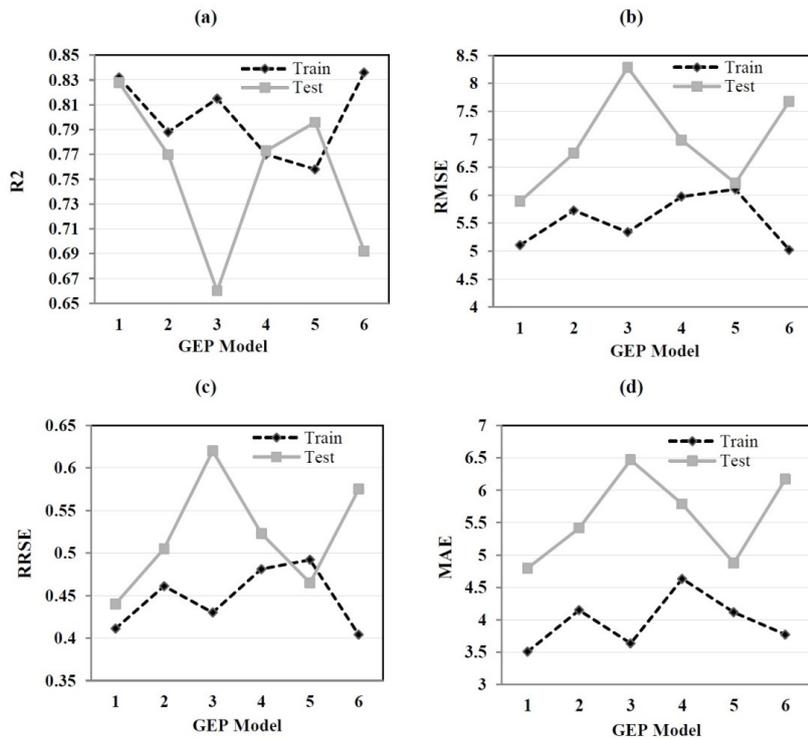

Fig. 8- Comparison of validation GEP models criteria (a) R^2, (b) RMSE, (c) RRSE, (d) MAE for GEP-I structure.
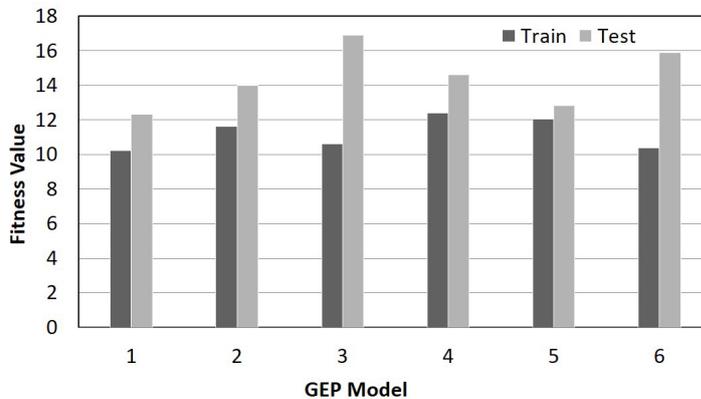

Fig. 9- The changes in fitness values as a function of generation number for various GEP models.
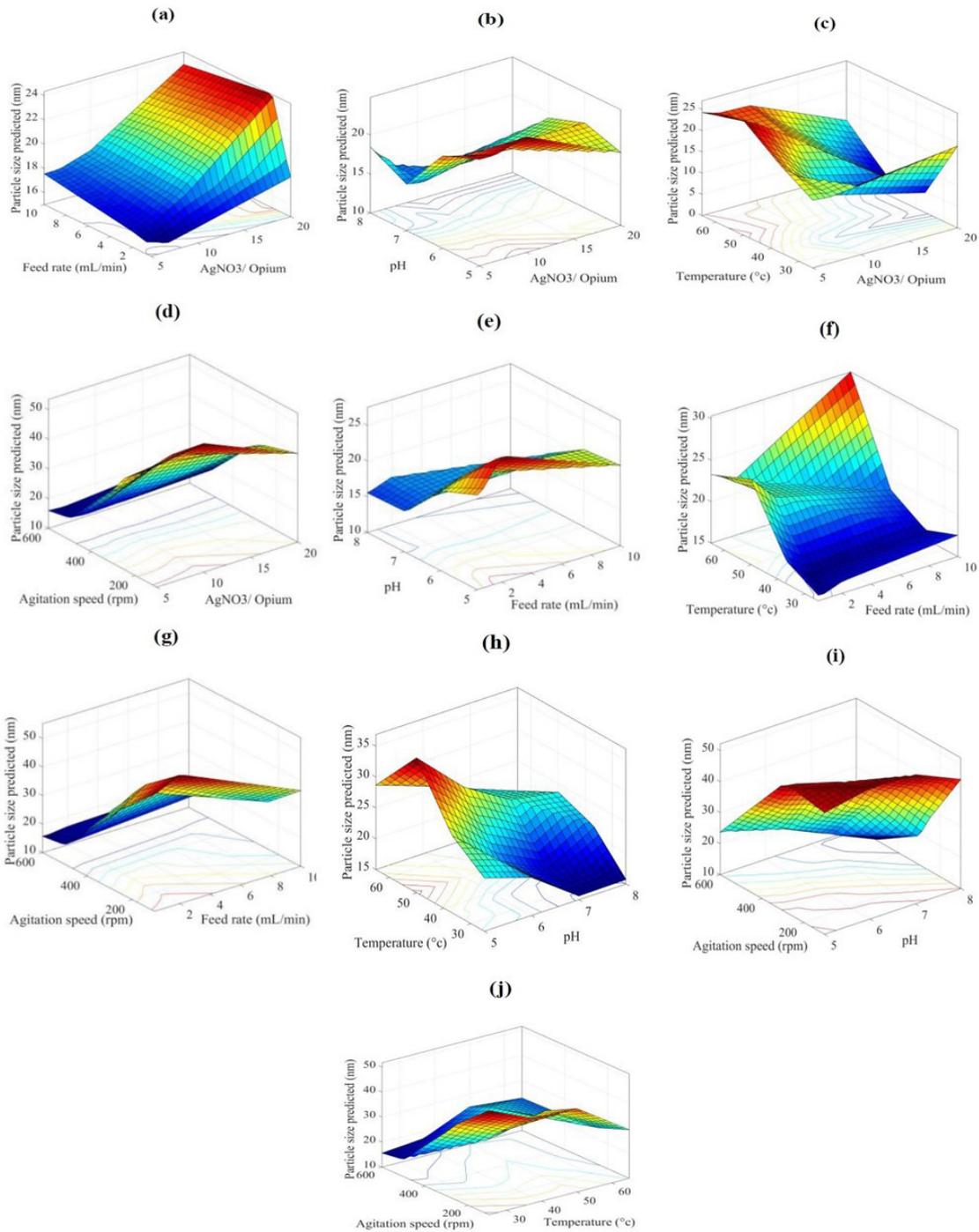
Fig. 10- An example of 3-dimensional changes of operational variables by AgNPs size; (a) of AgNO$_3$/OS versus feeding rate, (b) AgNO$_3$/OS versus pH, (c) AgNO$_3$/OS versus T, (d) AgNO$_3$/OS versus AS, (e) pH versus feeding rate, (f) T versus feeding rate, (g) AS versus feeding rate, (h) T versus pH, (i) AS versus pH, (j) AS versus T.

effect of two parameters in reducing the size of AgNPs in aqueous zones has been shown and explained based on it. The interaction of the parameters, AgNO$_3$ with OS, and the amount of Fr cannot be independently explained because, as

shown in Figure 10 (a), the minimum parameters are required for the minimum size. If this ratio is high or low, it means an increase in one of the parameters. The role of silver nitrate is to supply reduces silver (Ag$^+$) ions. The role of the extract is to

accelerate the reduction of these ions to the metallic silver (Ag^0); hence, a balance must be struck, and this balance is not possible except by optimizing both parameters. In all reactions, the total reaction time is 30 min, and the concentration of silver nitrate is 1 mM. Therefore, if the amount of feeding time increases, more value from Ag^+ is converted to Ag^0. However, the role of these parameters must be optimized, taking into account the other parameters, and cannot be judged independently.

As shown in Figures 10 (b, e, h, i), increasing the pH of the solution leads to the formation of small nanoparticles. These results are consistent with the previous studies on the inverse relationship between AgNPs and pH. On the other hand, increasing the pH of the solution leads to the formation of spherical nanoparticles. In general, the pH of the solution affects the chemistry of the nanoparticles and balances the nucleation and growth process in them. Stimulation rate plays an important role in the size of nanoparticles and the placement of silver ions in the presence of reducing agents (Figures 10 (c, f, h, j)).

Experimental results showed that a high excitation rate, with an increase in the reaction level, leads to a more homogeneous environment and smaller nanoparticles. On the other hand, particle size reduction and narrow size distribution with increasing T are known phenomena. The reason is to control the reaction kinetics. The reaction rate is slow at low T, while at higher T, particle formation and growth are complete, and the consumption of silver ions increases. But it should be noted that with increasing the pH of the solution, the T is low. The reason is the change in the chemical nature of the reaction with the increase of this parameter, and if the T is high, the particle size occurs due to the binding and accumulation of particles.

By consideration of green synthesis as an extensive approach for the preparation of AgNPs,

the general trend including the positive or negative effect of each experimental parameter on the size of AgNPs was investigated, separately [26-33]. The results mentioned above are in good agreement with previous studies on the effectiveness of these parameters and their role on the size of AgNPs. Generally, the prediction of AgNPs the effect of five variables, including $AgNO_3$/OS, AS, Fr, pH, and T, were studied.

By using sensitivity analysis, the effect of experimental parameters on the size of AgNPs was considered by OS (Figure 11). Accordingly, the most important parameters in the size of AgNPs were Fr, $AgNO_3$ to OS ratio, and AS. It should be noted that the effect of the parameters should be considered together, and this does not mean that the effect of T and pH are negligible.

5. Conclusions

Today, the use of AgNPs is increasing, especially in medical applications. It may because of its small size, leading to an increase in the effective level and greater effectiveness due to the relationship between size and morphology. This study is the first study that used GEP to model the size of AgNPs prepared by green synthesis that uses OS as a reducing agent. Six user-friendly GEP models are constructed for the estimation of the size of AgNPs as a function of $AgNO_3$/OS ratio, as a reducing agent, AS, Fr, pH, and T. By random distribution, 25% of selected data set employed for testing, and remained 75% were used in training steps. In order to obtain the best GEP model with minimum error and maximum R^2, a series of analyses were performed using the fitness value procedure, and finally, GEP-I with 0.828 R^2, 0.44 RRSE, 5.894 RMSE, and 4 was proposed as appropriate GEP model. It has 3 genes, 8 heads, and 30 chromosomes, which can be the very best training algorithm and presents a worthy performance for GEP modeling of the size
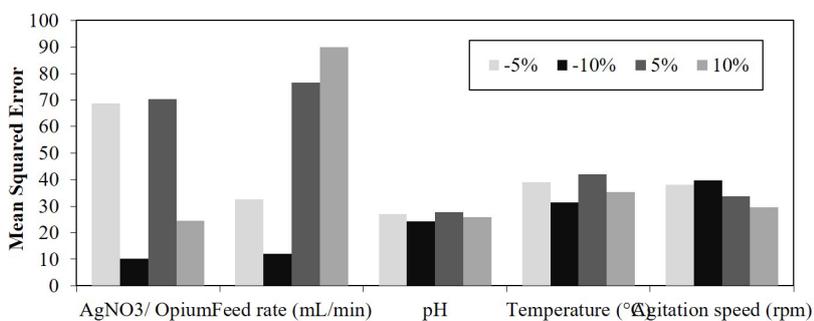

Fig. 11- Effect of input variables in the size of AgNPs.

of AgNPs. According to the results of this research, it could be suggested that genetic programming models can be used for the size prediction of AgNPs. The results of sensitivity analysis reveal that the $AgNO_3$-to-OS ratio and feeding rate are the most effective parameters, and the pH of the reaction is the least effective parameter on AgNPs size.

References

1. Mishra AK, Tiwari KN, Saini R, Kumar P, Mishra SK, Yadav VB, et al. Green Synthesis of Silver Nanoparticles from Leaf Extract of Nyctanthes arbor-tristis L. and Assessment of Its Antioxidant, Antimicrobial Response. Journal of Inorganic and Organometallic Polymers and Materials. 2019;30(6):2266-78.

2. Rana A, Yadav K, Jagadevan S. A comprehensive review on green synthesis of nature-inspired metal nanoparticles: Mechanism, application and toxicity. Journal of Cleaner Production. 2020;272:122880.

3. Khan I, Saeed K, Khan I. Nanoparticles: Properties, applications and toxicities. Arabian Journal of Chemistry. 2019;12(7):908-31.

4. Bhagat M, Anand R, Datt R, Gupta V, Arya S. Green Synthesis of Silver Nanoparticles Using Aqueous Extract of Rosa brunonii Lindl and Their Morphological, Biological and Photocatalytic Characterizations. Journal of Inorganic and Organometallic Polymers and Materials. 2019;29(3):1039-47.

5. Duan H, Wang D, Li Y. Green chemistry for nanoparticle synthesis. Chem Soc Rev. 2015;44(16):5778-92.

6. Das RK, Pachapur VL, Lonappan L, Naghdi M, Pulicharla R, Maiti S, et al. Biological synthesis of metallic nanoparticles: plants, animals and microbial aspects. Nanotechnology for Environmental Engineering. 2017;2(1).

7. Thakkar KN, Mhatre SS, Parikh RY. Biological synthesis of metallic nanoparticles. Nanomedicine. 2010;6(2):257-62.

8. Hooman Khademi MD, Farin Kamangar MD, Paul Brennan MD, Reza Malekzadeh MD. Opioid therapy and its side effects: a review. Archives of Iranian medicine. 2016 Dec;19(12):870.

9. Pathan H, Williams J. Basic opioid pharmacology: an update. Br J Pain. 2012;6(1):11-6.

10. Schiff PL. Opium and its alkaloids. American Journal of Pharmaceutical Education. 2002 Jan;66(2):188-96.

11. Sattari R, Khayati G. Prediction of the size of silver nanoparticles prepared via green synthesis: A gene expression programming approach. Scientia Iranica. 2020;0(0):0-.

12. McClelland JL, Rumelhart DE. Parallel Distributed Processing: The MIT Press; 1986.

13. Liu SW, Huang JH, Sung JC, Lee CC. Detection of cracks using neural networks and computational mechanics. Computer Methods in Applied Mechanics and Engineering. 2002;191(25-26):2831-45.

14. Anderson JA. Cognitive and psychological computation with neural models. IEEE Transactions on Systems, Man, and Cybernetics. 1983;SMC-13(5):799-815.

15. Gregory NW. Elements of X-Ray Diffraction. Journal of the American Chemical Society. 2002;79(7):1773-4.

16. Khayati GR, Janghorban K, Shariat MH. Isothermal kinetics of mechanochemically and thermally synthesized Ag from Ag2O. Transactions of Nonferrous Metals Society of China. 2012;22(4):935-42.

17. shafaei A, Khayati GR. A predictive model on size of silver nanoparticles prepared by green synthesis method using hybrid artificial neural network-particle swarm optimization algorithm. Measurement. 2019;151:107199.

18. Nazari A. Compressive strength of geopolymers produced by ordinary Portland cement: Application of genetic programming for design. Materials & Design. 2012;43:356-66.

19. Modified Particle Swarm Optimization-Artificial Neural Network and Gene Expression Programing for Predicting High Temperature Oxidation Behavior of Ni–Cr–W-Mo Alloys. International Journal of Engineering. 2020;33(11).

20. . Nuclear Instruments and Methods in Physics Research Section A: Accelerators, Spectrometers, Detectors and Associated Equipment. 2005;551(1):ix.

21. Koza J. Genetic programming as a means for programming computers by natural selection. Statistics and Computing. 1992;4(2).

22. Ashour AF, Alvarez LF, Toropov VV. Empirical modelling of shear strength of RC deep beams by genetic programming. Computers & Structures. 2003;81(5):331-8.

23. Eskil M, Kanca E. A new formulation for martensite start temperature of Fe–Mn–Si shape memory alloys using genetic programming. Computational Materials Science. 2008;43(4):774-84.

24. Hoseinian FS, Faradonbeh RS, Abdollahzadeh A, Rezai B, Soltani-Mohammadi S. Semi-autogenous mill power model development using gene expression programming. Powder Technology. 2016;308:61-9.

25. Mahdavi Jafari M, Khayati GR. Prediction of hydroxyapatite crystallite size prepared by sol–gel route: gene expression programming approach. Journal of Sol-Gel Science and Technology. 2018;86(1):112-25.

26. Alqadi MK, Abo Noqtah OA, Alzoubi FY, Alzouby J, Aljarrah K. pH effect on the aggregation of silver nanoparticles synthesized by chemical reduction. Materials Science-Poland. 2014;32(1):107-11.

27. Phanjom P, Ahmed G. Effect of different physicochemical conditions on the synthesis of silver nanoparticles using fungal cell filtrate of Aspergillus oryzae (MTCC No. 1846) and their antibacterial effect. Advances in Natural Sciences: Nanoscience and Nanotechnology. 2017;8(4):045016.

28. Junaidi, Yunus M, Harsojo, Suharyadi E, Triyana K. Effect of Stirring rate on The Synthesis Silver Nanowires using Polyvinyl Alcohol as A Capping Agent by Polyol Process. International Journal on Advanced Science, Engineering and Information Technology. 2016;6(3):365.

29. Kasture MB, Patel P, Prabhune AA, Ramana CV, Kulkarni AA, Prasad BLV. Synthesis of silver nanoparticles by sophorolipids: Effect of temperature and sophorolipid structure on the size of particles. Journal of Chemical Sciences. 2008;120(6):515-20.

30. Jiang XC, Chen WM, Chen CY, Xiong SX, Yu AB. Role of Temperature in the Growth of Silver Nanoparticles Through a Synergetic Reduction Approach. Nanoscale Res Lett. 2011;6(1):32.

31. Peer Review #1 of "Green synthesis of silver nanoparticles in aloe vera plant extract prepared by a hydrothermal method and their synergistic antibacterial activity (v0.1)". PeerJ; 2015.

32. Pris M. Influence of different parameters on wet synthesis of silver nanoparticles (Bachelor's thesis, University of Twente).

33. Vanaja M, Rajeshkumar S, Paulkumar K, Gnanajobitha G, Malarkodi C, Annadurai G. Kinetic study on green synthesis of silver nanoparticles using Coleus aromaticus leaf extract. Adv. Appl. Sci. Res. 2013;4(3):50-5.